

# Hadron–Resonance Gas at Freeze–out: Reminder on Importance of Repulsive Interactions

V.V. Begun,<sup>1,2</sup> M. Gaździcki,<sup>2,3</sup> and M.I. Gorenstein<sup>1,4</sup>

<sup>1</sup>*Bogolyubov Institute for Theoretical Physics, Kiev, Ukraine*

<sup>2</sup>*Institut für Kernphysik, Goethe–Universität, Frankfurt am Main, Germany*

<sup>3</sup>*Instytut Fizyki, Jan Kochanowski University, Kielce, Poland*

<sup>4</sup>*Frankfurt Institute for Advanced Studies, Frankfurt am Main, Germany*

## Abstract

An influence of the repulsive interactions on matter properties is considered within the excluded volume van der Waals hadron-resonance gas model. Quantitative results are presented for matter at the chemical freeze-out in central nucleus-nucleus collisions at relativistic energies. In particular, it is shown that repulsive interactions connected to non-zero size of created particles lead to a significant decrease of collision energy at which the net-baryon density has a maximum. A position of the transition point from baryon to meson dominated matter depends on the difference between baryon and meson hard-core radiuses.

PACS numbers: 12.40.-y, 12.40.Ee

Keywords: hadron-resonance gas, nucleus-nucleus collisions, chemical freeze-out, compressed baryonic matter, repulsive interactions, van der Waals excluded volume model

## I. INTRODUCTION

Statistical models of the hadron gas are an important tool to extract properties of matter created in relativistic nucleus-nucleus collisions (see, e.g., Refs. [1–7]). Basic parameters of these models are the matter temperature  $T$ , baryon chemical potential  $\mu_B$ , and volume  $V$ . If supplemented by additional model parameters monitoring deviations from the chemical equilibrium [8], they approximately fit rich data on mean hadron multiplicities in a broad range of reactions, from  $e^+e^-$ ,  $p+p$ , and  $p+\bar{p}$  [9] at low energies to central Pb+Pb collisions at the highest LHC energy [10].

The most popular version of the statistical models of hadron matter is the ideal hadron-resonance gas (I–HRG), i.e., a statistical system of non-interacting hadrons and resonances. It is argued, based on the Dashen, Ma and Bernstein theorem [11], that resonances introduced to the ideal hadron gas take into account attractive interactions between hadrons. The repulsive part of the interactions between hadrons is usually accounted for by the van der Waals excluded volume procedure generalized to the relativistic case of a variable number of hadrons [12]. The resulting excluded volume model is no longer an ideal gas model, and in this paper it will be denoted as the EV–HRG model. Another popular example of modelling attractive and repulsive interactions between hadrons is the relativistic mean field theory in a form of the Walecka model [13] and its different modifications (see e.g., the recent paper [14] and references therein). In this approach, scalar and vector meson fields describe respectively the attractive and repulsive forces between baryons.

Both the attractive and repulsive interactions are important for the qualitative as well as quantitative description of the properties of strongly interacting matter. For example, the nucleon-nucleon potential includes both parts – attractive at large and repulsive at small distances. The presence of both attractive and repulsive interactions between nucleons is crucial for the existence of stable nuclei. Moreover, an important undesired feature of the I–HRG model at high temperatures was noted by the authors of Refs. [15, 16]. Due to the large number of different types of baryons and mesons, the point-like hadrons would always become the dominant phase at very high energy density. Just the excluded volume effects ensure a transition from a gas of hadrons and resonances to the quark-gluon plasma. Thus, one needs the

EV–HRG equation of state for hydrodynamic models of nucleus-nucleus collisions (see, e.g., Refs. [17–19]). Note that the lattice QCD calculations also indicate a presence of excluded volume corrections [20].

The aim of this paper is to recall the role of repulsive interactions between hadrons. It is shown that the excluded volume hadron-resonance gas model yields different properties of matter at the freeze-out than the ideal hadron-resonance gas, if densities and their collision energy dependence are considered. Quantitative results are presented for two examples, namely collision energy dependence of the net-baryon density [21] as well as the ratio of baryon and meson entropy density [22–24]. They are selected, because of conjectures that the maximum of net-baryon density as well as the transition between baryon and meson dominated matter may be related to the onset of deconfinement observed in central Pb+Pb collisions at the CERN SPS energies [25]. Note that chemical freeze-out parameters  $T$  and  $\mu_B$  in nucleus-nucleus collisions are straightforwardly connected to the data on hadron multiplicities. The energy range considered in this paper is presently studied experimentally at the CERN SPS [26] and the BNL RHIC [27]. In future this effort will be extended by experiments at new accelerators, at the JINR NICA [28] and the FAIR SIS–100 [29–31].

The paper is organized as follows. In Sec. II the ideal hadron-resonance gas model is introduced. The excluded volume hadron-resonance gas model is presented in Sec. III, where also quantitative results for densities at the chemical freeze-out in central Pb+Pb collisions are given and discussed. A summary given in Sec. IV closes the paper.

## II. IDEAL HADRON–RESONANCE GAS

In the grand canonical ensemble the pressure of the I–HRG is given by

$$p^{id} = \sum_i p_i^{id}(T, \mu_i) = \sum_i \frac{d_i}{6\pi^2} \int_0^\infty \frac{k^4 dk}{(k^2 + m_i^2)^{1/2}} \left[ \exp\left(\frac{\sqrt{k^2 + m_i^2} - \mu_i}{T}\right) + \eta \right]^{-1}, \quad (1)$$

where  $T$  is the system temperature,  $\eta = -1$  and  $\eta = 1$  for bosons and fermions, respectively, while  $\eta = 0$  corresponds to the Boltzmann approximation. For a hadron  $i$ ,  $m_i$  is its mass and  $d_i$  is the spin degeneracy. The chemical potential is given by

$$\mu_i = b_i \mu_B + s_i \mu_S + q_i \mu_Q \quad (2)$$

with  $b_i = 0, \pm 1$ ,  $s_i = 0, \mp 1, \mp 2, \mp 3$  and  $q_i = 0, \pm 1, \pm 2$  for hadrons. The number density of a hadron  $i$  reads:

$$n_i^{id}(T, \mu_i) = T \frac{\partial p^{id}}{\partial \mu_i} = \frac{d_i}{2\pi^2} \int_0^\infty k^2 dk \left[ \exp \left( \frac{\sqrt{k^2 + m_i^2} - \mu_i}{T} \right) \pm 1 \right]^{-1}. \quad (3)$$

Considering the temperature  $T$ , baryon chemical potential  $\mu_B$ , and volume  $V$  as free parameters one can fit mean hadron multiplicities  $\langle N_i \rangle = V n_i$  measured in relativistic nucleus-nucleus collisions at each collision energy. In this analysis,  $\mu_S$  and  $\mu_Q$  are expressed as functions of  $T$  and  $\mu_B$  when the conditions on strangeness,  $\langle S \rangle = 0$ , and electric to baryon charge ratio,  $\langle Q \rangle / \langle B \rangle = Z/A$ , are taken into account. Most of experimental data on nucleus-nucleus collisions concern yields of long-lived hadrons, which include products of resonance decays. This requires a proper treatment of short-lived resonances, namely the products of their strong and electromagnetic decays should be added to the mean multiplicities of stable hadrons. In this paper the numerical implementation of the hadron-resonance gas model provided by the THERMUS package [32] is used to calculate the relevant quantities according to Eqs. (4-7). Particles and resonances [all mesons up to  $K_4^*(2045)$ ] and baryons (up to  $\Omega^-$ ), quantum statistics, as well as the width of resonances are included.

The analysis of central Pb+Pb (Au+Au) collisions registered by experiments at SIS, AGS, SPS, and RHIC allows to establish the collision energy dependence of  $T$  and  $\mu_B$  which can be parameterized as [23]:

$$T = 0.166 \text{ GeV} - 0.139 \text{ GeV}^{-1} \mu_B^2 - 0.053 \text{ GeV}^{-3} \mu_B^4, \quad (4)$$

$$\mu_B = \frac{1.308 \text{ GeV}}{1 + 0.273 \text{ GeV}^{-1} \sqrt{s_{NN}}}, \quad (5)$$

where  $\sqrt{s_{NN}}$  is the center-of-mass energy of a nucleon pair. The chemical freeze-out line,  $T = T(\mu_B)$ , as well as the energy dependence of the  $T$  and  $\mu_B$  parameters are shown in Figs. 1 (a) and (b), respectively.

The net-baryon density  $\rho_B$ , entropy density  $s$ , and energy density  $\varepsilon$  can be found from the system pressure  $p$  using the thermodynamical relations:

$$\rho_B = \frac{\partial p}{\partial \mu_B}, \quad s = \frac{\partial p}{\partial T}, \quad \varepsilon = T \frac{\partial p}{\partial T} + \mu \frac{\partial p}{\partial \mu} - p. \quad (6)$$

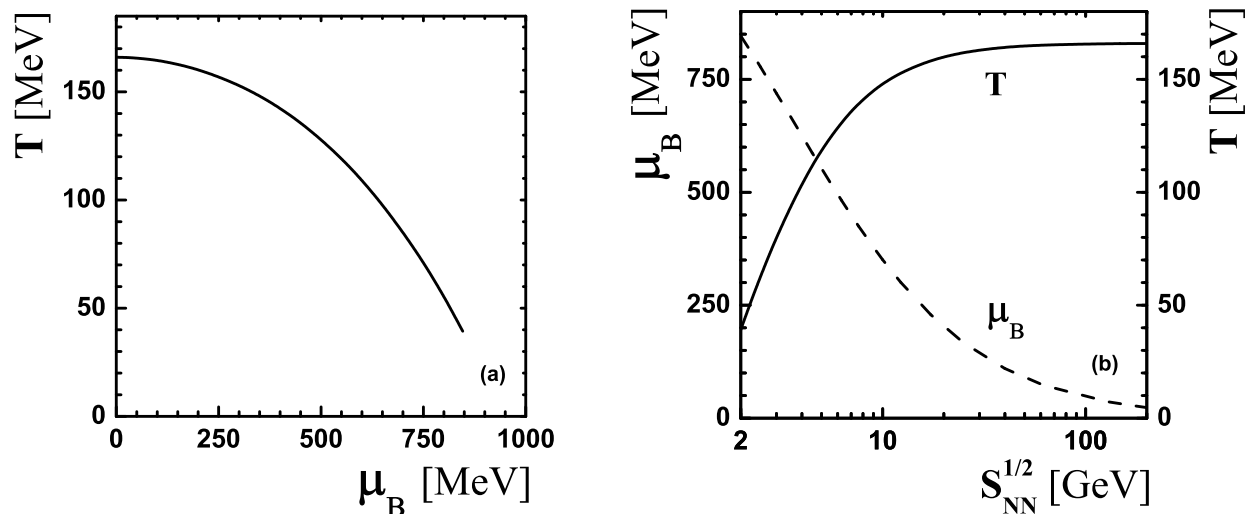


FIG. 1: (Color online) (a): The chemical freeze-out line  $T = T(\mu_B)$ . (b): The  $T$  and  $\mu_B$  along the chemical freeze-out as a function of  $\sqrt{s_{NN}}$ .

With the chemical freeze-out parameters given by Eq. (4) and the ideal gas expression Eq. (1) for the system pressure, one finds the quantities in Eq. (6) as functions of the collision energy. The I-HRG model is based on the assumption of complete thermal and chemical equilibrium. An additional I-HRG parameter, the strangeness suppression factor  $\gamma_S$ , has to be introduced to account for deviations of strange hadron multiplicities from chemical equilibrium [8]. Its dependence on  $T$  and  $\mu_B$  obtained by fitting hadron yields measured in the full phase space can be parameterized as [7]

$$\gamma_S = 1 - 0.396 \exp\left(-1.23 \frac{T}{\mu_B}\right). \quad (7)$$

At the AGS and SPS energies the  $\gamma_S$  parameter is significantly smaller than 1, which means the under-saturation of strange hadron yields with respect to the chemical equilibrium. The  $\gamma_S$  parameter should be included in the model if a proper description of strange hadron yields is required. However, the relation between  $T$  and  $\mu_B$  as well as the chemical freeze-out line Eq. (4), obtained within the models with and without the  $\gamma_S$  parameter, is similar.

The net-baryon density  $\rho_B^{id}$  as a function of collision energy calculated following the freeze-out line (4) is shown in Fig. 2 (a). In this and the following figures the laboratory collision energy per

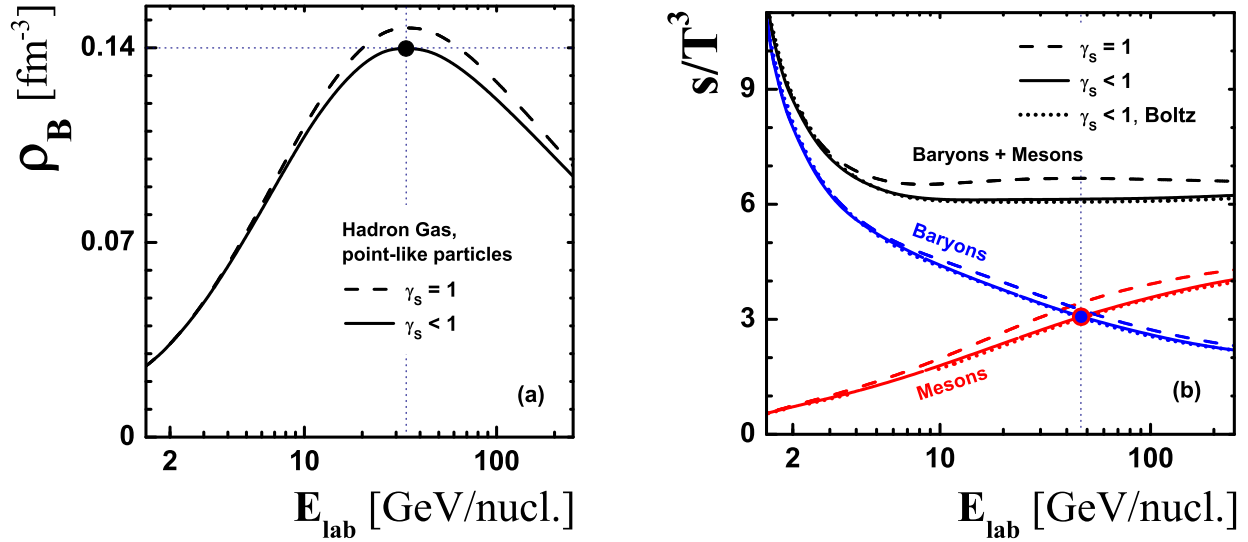


FIG. 2: (Color online) The (a) net-baryon density  $\rho_B$  and (b) the ratio  $s/T^3$  along the chemical freeze-out line Eq. (4) and  $\gamma_s$  according to Eq. (7) are shown by the solid lines. The dashed lines correspond to  $\gamma_s = 1$  for (a)  $\rho_B$  and (b)  $s/T^3$ . The dotted line corresponds to the Boltzmann approximation in  $s/T^3$ .

projectile nucleon  $E_{lab}$  is used to present the dependence on collision energy. Its connection to center-of-mass energy per nucleon pair,  $\sqrt{s_{NN}}$ , is given by  $\sqrt{s_{NN}} = \sqrt{2m_N E_{lab} + 2m_N^2}$ , where  $m_N$  is the nucleon mass. As seen in Fig. 2 (a), the net-baryon density has a maximum [21] at  $E_{lab} \cong 34A$  GeV. This is the collision energy at which the NA49 Collaboration observed the maximum of the  $K^+/\pi^+$  ratio (the *horn*) and other signals of the onset of deconfinement [25].

The total entropy density as a function of collision energy following the freeze-out line Eq. (4) is shown in Fig. 2 (b). Meson  $s_M$  and baryon  $s_B$  entropy densities are also presented in the figure. With increasing collision energy the baryon-dominated ( $s_B > s_M$ ) matter changes to meson-dominated ( $s_M > s_B$ ) matter. For the I-HRG model this transition is located at  $E_{lab} \cong 46A$  GeV.

For the  $T-\mu_B$  values at the chemical freeze-out line Eq. (4) the role of quantum statistics is small. For baryons the Fermi statistics changes their densities by less than 1%. The largest density change due to the Bose statistics is for pions. It is, however, still smaller than 10%.

The ratio  $s/T^3$  calculated within the Boltzmann approximation, i.e.  $\eta = 0$  in Eq. (1), is shown in Fig. 2 (b) by the dotted line. The deviations from the results with quantum statistics included are hardly visible. They are even smaller for  $\rho_B$  and thus the corresponding dotted line calculated with the Boltzmann approximation is not plotted. The collision energy dependence of  $\rho_B$  and  $s/T^3$  calculated for the  $\gamma_S$  parametrization Eq. (7) and for  $\gamma_S = 1$  is also shown in Fig. 2. One concludes that the energy at which  $\rho_B$  has the maximum as well as the energy of the transition between baryon-dominated and meson-dominated matter are approximately independent of the quantum statistics and the degree of strangeness equilibration.

It was suggested [22] that the maximum of the net-baryon density and/or the transition from baryon to meson dominance may be related to the anomalous behavior of the  $K^+/\pi^+$  ratio [25]. In the next section these phenomena are examined by taking into account the repulsive interactions between hadrons.

### III. EXCLUDED VOLUME HADRON-RESONANCE GAS

The results presented in Section II have been obtained within the ideal hadron-resonance gas model in which only attractive interactions between hadrons are taken into account by the inclusion of resonances. In this section the role of repulsive interactions is considered within the excluded volume hadron-resonance gas model.

The van der Waals excluded volume procedure corresponds to a substitution of the system volume  $V$  by the available volume  $V_{\text{av}}$ ,

$$V \rightarrow V_{\text{av}} = V - \sum_i v_i N_i, \quad (8)$$

where  $v_i = 4 \cdot (4\pi r_i^3/3)$  is the excluded volume parameter and  $r_i$  is the corresponding hard sphere radius of a particle  $i$ . This result, in particular, the presence of a factor of 4 in the expression for  $v_i$ , can be rigorously obtained for a low density gas of particles of a single type (see, e.g., Ref. [33]). In the grand canonical ensemble, the substitution (8) leads to a

transcendental equation for the pressure of the EV-HRG<sup>1</sup> [12, 15]:

$$p = \sum_i p_i^{id}(T, \tilde{\mu}_i) ; \quad \tilde{\mu}_i = \mu_i - v_i p . \quad (9)$$

Using Eq. (6) one finds the net-baryon, entropy and energy densities:

$$\rho_B = \frac{\sum_i b_i n_i^{id}(T, \tilde{\mu}_i)}{1 + \sum_j v_j n_j^{id}(T, \tilde{\mu}_j)} , \quad s = \frac{\sum_i s_i^{id}(T, \tilde{\mu}_i)}{1 + \sum_j v_j n_j^{id}(T, \tilde{\mu}_j)} , \quad \varepsilon = \frac{\sum_i \varepsilon_i^{id}(T, \tilde{\mu}_i)}{1 + \sum_j v_j n_j^{id}(T, \tilde{\mu}_j)} . \quad (10)$$

In comparison to the corresponding densities calculated within the I-HRG model the densities in the EV-HRG model Eq. (10) are lower because of two reasons:

- i) due to the suppression factor  $[1 + \sum_j v_j n_j^{id}(T, \tilde{\mu}_j)]^{-1}$  and
- ii) due to the shift in chemical potential  $\mu_i \rightarrow \tilde{\mu}_i$  which in the Boltzmann approximation leads to the suppression factor  $\exp(-v_i p/T) < 1$ .

The shift of the chemical potential makes the Boltzmann approximation even more accurate than in the case of the ideal gas. If all proper volume parameters are the same  $v_i = v$  (i.e.  $r_i = r$ ), the Boltzmann approximation gives the total suppression factor  $R$

$$R(T, \mu_B; r) = \frac{\exp(-v p/T)}{1 + v \sum_j n_j^{id}(T, \tilde{\mu}_j)} , \quad (11)$$

the same for all densities of Eq. (10):

$$\rho_B(T, \mu_B) = R \rho_B^{id}(T, \mu_B) , \quad s(T, \mu_B) = R s^{id}(T, \mu_B) , \quad \varepsilon(T, \mu_B) = R \varepsilon^{id}(T, \mu_B) \quad (12)$$

and  $n_i(T, \mu_B) = R n_i^{id}(T, \mu_B)$ . Typical values of hard-core radii considered in the literature [2, 17, 18, 20, 35] are  $r = (0.3 \div 0.8)$  fm.

The energy dependence of the suppression factor Eq. (11) calculated along the chemical freeze-out line for  $r = 0.5$  fm and  $r = 1$  fm is shown in Fig. 3 (a). The  $R$  factor (11) decreases monotonously with increasing collision energy. For example, for  $r = 0.5$  fm one finds  $R \cong 0.9$  and  $R \cong 0.4$  at small and large  $E_{lab}$ , respectively. One may therefore expect a decrease of the value of  $\rho_B$  at its maximum by a factor of 0.5 (for  $r = 0.5$  fm), and a shift of the position of the maximum to a smaller collision energy. In fact, in Fig. 4 (a) one observes that the maximum of the net-baryon density is located at  $E_{lab} \cong 17A$  GeV for  $r = 0.5$  fm and at  $E_{lab} \cong 7A$  GeV

---

<sup>1</sup> A discussion of other excluded volume formulations can be found in Ref. [34].



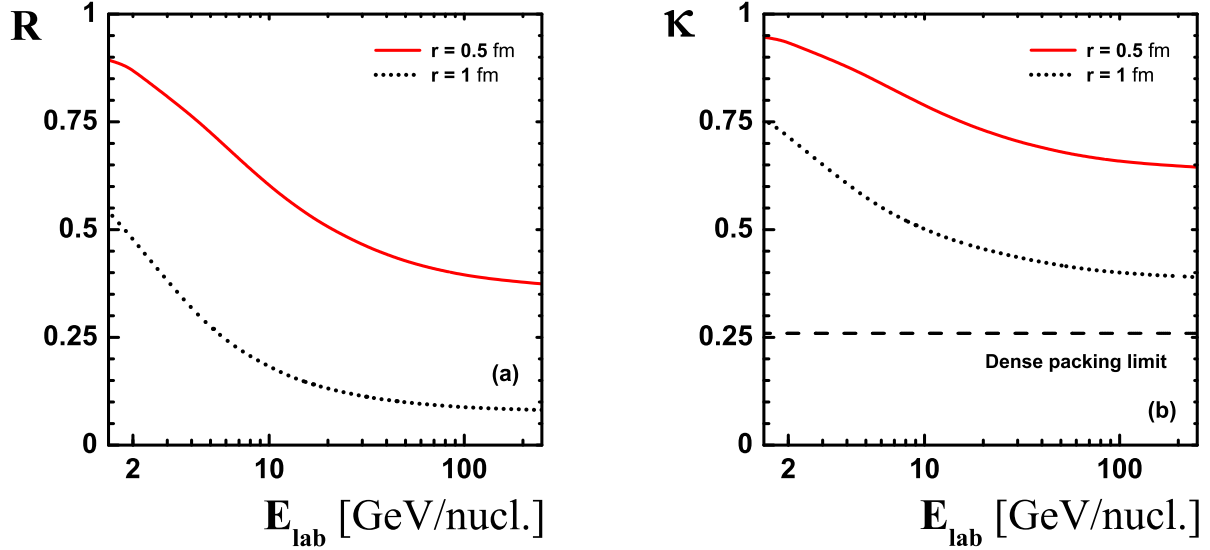


FIG. 3: (Color online) (a) The excluded volume suppression factor  $R$  Eq. (11) and (b) the fraction of the available volume  $\kappa$  Eq. (13) as functions of  $E_{lab}$  along the chemical freeze-out line Eqs. (4) and (7). The solid and dotted lines correspond to  $r = 0.5$  fm and  $r = 1$  fm, respectively. The dashed line in (b) corresponds to the dense packing limit 0.26 for hard spheres.

for  $r = 1$  fm, instead of  $E_{lab} \cong 34A$  GeV for the I-HRG model. It is also seen that the value of  $\rho_B$  at the maximum decreases strongly with the increasing value of the hard-core radius. The entropy density shown in Fig. 4 (b) is reduced by the same suppression factor. The collision energy at which the baryon and meson entropy densities are equal is, however, independent of  $R$  and is located at  $E_{lab} \cong 46A$  GeV. This is however true only if the hard-core radius  $r$  is the same for all hadrons.

A fraction of the total volume  $\kappa \equiv V_{av}/V$ , which is available for the extended hadrons, can be estimated as follows for equal baryon and meson radiuses:

$$\kappa = \frac{V - v \sum_i N_i}{V} = 1 - v \sum_i n_i(T, \tilde{\mu}_i) = 1 - \frac{v \sum_i n_i^{id}(T, \tilde{\mu}_i)}{1 + v \sum_j n_j^{id}(T, \tilde{\mu}_j)} = \exp\left(\frac{vp}{T}\right) R. \quad (13)$$

The parameter  $\kappa$  is shown in Fig. 3 (b) for  $r = 0.5$  and  $r = 1$  fm. One can see that  $\kappa$  is always larger than the dense packing limit for hard spheres:  $1 - \pi/(3\sqrt{2}) \cong 0.26$  [33]. This ensures a consistency of the excluded volume approach at all collision energies even for the largest

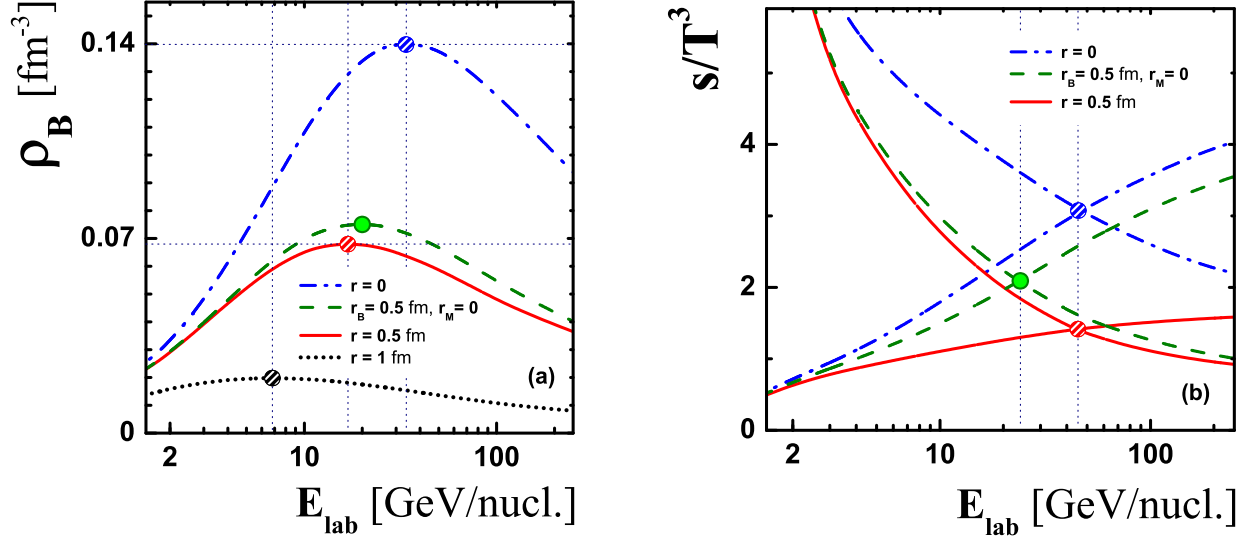


FIG. 4: (Color online) (a): The net-baryon density along the chemical freeze-out line from Eqs. (4) and (7). Dashed-dotted line corresponds to the model with  $r = 0$ , dashed line to  $r_B = 0.5 \text{ fm}$  and  $r_M = 0$ , solid line to  $r_B = r_M = r = 0.5 \text{ fm}$ , and dotted line to  $r_B = r_M = r = 1 \text{ fm}$ . (b) The ratios  $s_B/T^3$  and  $s_M/T^3$  along the chemical freeze-out line Eqs. (4) and (7). Dashed-dotted lines correspond to the model with  $r = 0$ , solid lines to  $r_B = r_M = r = 0.5 \text{ fm}$ , and dashed-dotted lines to  $r_B = 0.5 \text{ fm}$  and  $r_M = 0$ .

considered radius  $r = 1 \text{ fm}$ . We also remind that the excluded volume parameter  $v$  is assumed to be four times larger than the hadron volume  $4\pi r^3/3$ .

It is interesting to consider the role of the excluded volume effects for different hard-core radii of baryons  $r_B$  and mesons  $r_M$ . As an example, the results for  $r_B = 0.5 \text{ fm}$  and  $r_M = 0$  are presented in Fig. 4. In a comparison to the results for  $r = 0.5 \text{ fm}$  for all hadrons one observes small changes of  $\rho_B$  but a significant shift of the transition point between the baryon and meson dominated matter. Its position decreases from  $E_{\text{lab}} \cong 46A \text{ GeV}$  to  $E_{\text{lab}} \cong 23A \text{ GeV}$ .

The model with non-equal hard-core radii ( $r_B = 0.7 \text{ fm}$  and  $r_M = 0$ ) was already used in Ref. [17]. The EV-HRG models with non-equal radii for different hadron species need, however, further detailed studies. This is because fits to the hadron yields performed with the EV-HRG model with non-equal radii give different freeze-out parameters  $T$  and  $\mu_B$  than those in Eq. (4)

obtained within the I-HRG model.

As an illustration, we estimate the possible changes of  $T$  and  $\mu_B$  freeze-out parameters due to the excluded volume effects with  $r_B \neq r_M$ . At least two particle ratios are required to determine  $T$  and  $\mu_B$ . In the presented examples these ratios are calculated using the parameters at the freeze-out line (4) obtained for  $r_B = r_M$ . Then using these ratios new freeze-out parameters  $T$  and  $\mu_B$  are calculated within the EV-HRG model with  $r_B = 0.5$  fm and  $r_M = 0$ . First, the pion to proton,  $\pi^+/p$ , and kaon to lambda,  $K^+/\Lambda$ , ratios are selected. These mesons and baryons are the most abundant particles. Second the  $\pi^+/p$  and  $K^-/\bar{\Lambda}$  ratios, which includes antibaryon, are considered. The results are shown in Fig. 5.

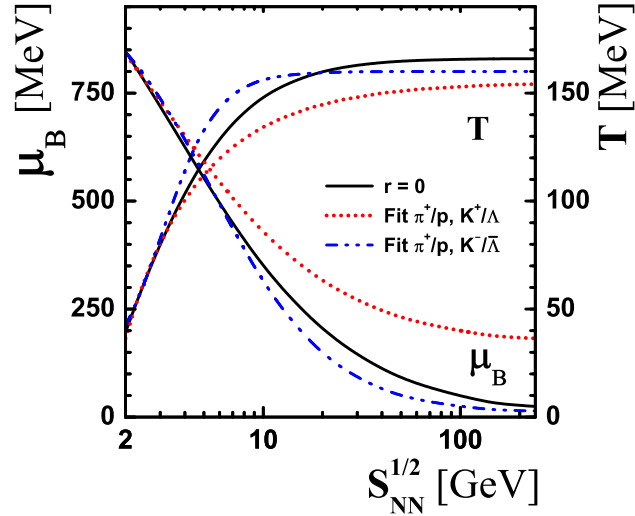


FIG. 5: (Color online) Comparison of the freeze-out line (4) (solid line), and the lines obtained using the  $\pi^+/p$ ,  $K^+/\Lambda$  (dotted line) and  $\pi^+/p$ ,  $K^-/\bar{\Lambda}$  ratios (dash-dotted line) within the EV-HRG model with  $r_B = 0.5 > r_M = 0$  fm. The ratios are calculated within I-HRG along the freeze-out line, Eq. (4), see text for details.

The new 'freeze-out lines' significantly deviate from the one obtained within the I-HRG model, Eq. (4). These deviations are also strongly dependent on the ratios or multiplicities selected for the analysis. For different reactions different hadron sets are measured with different precision. Therefore, accurate estimates of  $r_B$  and  $r_M$  from the data on hadron multiplicities would require a significant dedicated effort.

The baryon number density and baryon/meson entropy densities along the new freeze-out lines from Figs. 5 are shown in Fig. 6. The new fits with  $r_B = 0.5$  fm and  $r_M = 0$  change the

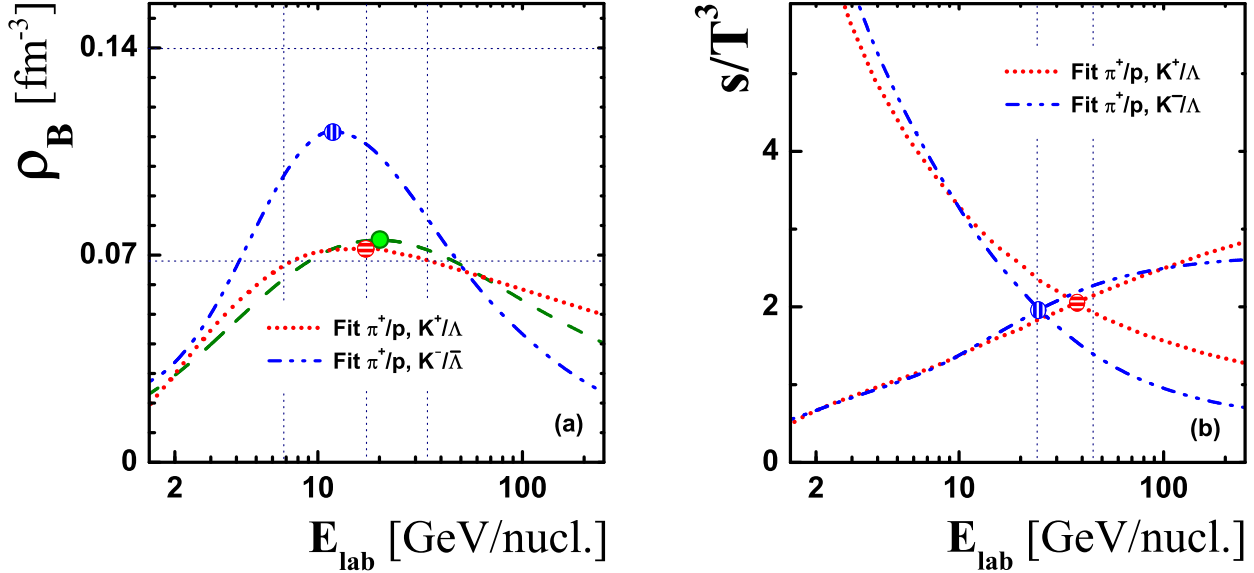


FIG. 6: (Color online) The same as in Fig. 4 for EV-HRG with  $r_B = 0.5 > r_M = 0$  fm. Dotted line corresponds to the fit of  $\pi^+/p$ ,  $K^+/\Lambda$  and dash-dotted line to the fit of the  $\pi^+/p$ ,  $K^-/\bar{\Lambda}$  ratios. Dashed line, vertical and horizontal dotted lines are the same as in Fig. 4.

details but preserve the main features of the system with  $r_B = r_M = 0.5$  fm. In particular, the position of the net-baryon density maximum depends basically on the  $r_B$  parameter while the position of the baryon/meson transition point is sensitive to the difference between the  $r_B$  and  $r_M$  parameters.

Particle number fluctuations are straightforwardly sensitive to the hard-core hadron radius  $r_B = r_M$  [36]. In a recent paper [37] the same freeze-out line as well as the THERMUS program has been used for the analysis of the event-by-event particle number fluctuations. Higher moments of the net-proton multiplicity distribution were calculated and compared with the STAR data. The results suggest that the hadron hard-core radius  $r_B = r_M$  is in the range from 0.3 fm to 0.5 fm. However, for the final conclusion the important effects of the exact charge conservation [38] and the experimental acceptance [39] should be also included and their consequences within the EV-HRG model should be studied.

#### IV. SUMMARY

The ideal hadron-resonance gas model is simple and has only a few free parameters. In spite of this it is successful in describing the bulk properties of mean hadron multiplicities in high energy collisions. The model takes into account attractive interactions between hadrons via a presence of resonances, but ignores repulsive interactions. The repulsive interactions are, however, needed to catch the basic qualitative features of strong interactions, e.g, the phase transition between hadron-resonance gas and the quark-gluon plasma: point-like hadrons and resonances would be a dominant phase at very high energy densities as their total degeneracy factor is much larger than that of quarks and gluons. Moreover, the repulsive interactions strongly modify the properties of the hadron-resonance gas. The most common way to include repulsive interactions in the hadron-resonance gas model is to follow the van der Waals excluded volume procedure and introduce the hard-core radii of hadrons.

If radii of all hadrons are assumed to be the same, the chemical freeze-out parameters, temperature and baryon chemical potential, fitted to data on mean hadron multiplicities are identical to those obtained within the ideal hadron-resonance gas model. However, all densities calculated within the van der Waals model are lower than the corresponding densities obtained within the ideal gas model and thus the fitted volume parameter in the van der Waals gas formulation is significantly larger. The density suppression factor  $R$  depends on the  $T$  and  $\mu_B$  parameters, which in turn depend on collision energy. Consequently, the collision energy dependence of densities is sensitive to the assumed hard-core radius of hadrons. In particular, the energy at which net-baryon density has a maximum decreases from about  $E_{lab} \cong 34A$  GeV for the ideal gas model to about  $E_{lab} \cong 7A$  GeV for the excluded volume model with  $r = 1$  fm. If the radii of hadrons are assumed to be different, the densities of different hadrons are modified differently. Clearly, the excluded volume effects are even larger for the hadron matter at stages preceding the chemical freeze-out in nucleus-nucleus collisions, i.e. at larger values of the energy density.

In view of these studies, the estimates of collision energies at which the net-baryon density at the chemical freeze-out reaches its maximum and/or the transition between baryon and meson dominated matter takes place are premature. One needs to renew a search for a suitable

set of the excluded volume parameters. Experimental and/or theoretical methods to better estimate hard-core radii of hadrons within the excluded volume model are needed to improve our understanding of the properties of hadron-resonance matter. If all hard-core radiuses are equal to each other, the particle number ratios are not sensitive to their numerical value. Thus, the data on average multiplicities are not enough and independent measurements of the total system volume is needed. However, the particle number fluctuations depend straightforwardly on the hard-core hadron radius [36]. Precise measurements of higher moments of hadron multiplicity distribution in nucleus-nucleus collisions are now in progress. An interpretation of these data within the EV-HRG opens the way to estimate the value of hard-core radius  $r$  from the data.

### Acknowledgments

We are thankful to W. Greiner, M. Hauer, Iu. Karpenko, L.M. Satarov, P. Seyboth, and V. Voronyuk for fruitful discussions. This work was supported by the Humboldt Foundation, by the Program of Fundamental Research of the Department of Physics and Astronomy of NAS, Ukraine, and by the German Research Foundation under Grant No. GA 1480/2-1 and the HICforFAIR Grant No. 20130403.

- 
- [1] J. Cleymans and H. Satz, Z. Phys. C **57**, 145 (1993).
  - [2] G. D. Yen, M. I. Gorenstein, W. Greiner, and S. N. Yang, Phys. Rev. C **56**, 2210 (1997); G. D. Yen and M. I. Gorenstein, Phys. Rev. C **59**, 2788 (1999).
  - [3] F. Becattini, J. Cleymans, A. Keranen, E. Suhonen and K. Redlich, Phys. Rev. C **64**, 024901 (2001).
  - [4] P. Braun-Munzinger, D. Magestro, K. Redlich, and J. Stachel, Phys. Lett. B **518**, 41 (2001).
  - [5] J. Rafelski and J. Letessier, Nucl. Phys. A **715**, 98c (2003).
  - [6] A. Andronic, P. Braun-Munzinger, and J. Stachel, Nucl. Phys. A **772**, 167 (2006).
  - [7] F. Becattini, J. Manninen and M. Gazdzicki, Phys. Rev. C **73**, 044905 (2006).
  - [8] J. Rafelski, Phys. Lett. **B262**, 333 (1991); P. Koch, B. Muller, J. Rafelski, Phys. Rep. **142**, 167 (1986). J. Letessier, J. Rafelski, A. Tounsi, Phys. Rev. **C50**, 406 (1994); C. Slotta, J. Sollfrank,

- U. Heinz, AIP Conf. Proc. (Woodbury) **340**, 462 (1995). J. Letessier and J. Rafelski, Phys. Rev. C **59**, 947 (1999) [hep-ph/9806386].
- [9] F. Becattini and U. W. Heinz, Z. Phys. C **76**, 269 (1997) [Erratum-ibid. C **76**, 578 (1997)] [hep-ph/9702274]; F. Becattini, Z. Phys. C **69**, 485 (1996).
- [10] M. Floris, J. Phys. G **38**, 124025 (2011) [arXiv:1108.3257 [hep-ex]]; A Kalweit [ALICE Collaboration], Acta Phys. Polon. B, Proc. Suppl. **5**, 225 (2012); B. Abelev *et al.* [ALICE Collaboration], arXiv:1202.1383 [hep-ex].
- [11] R. Dashen, S.-K. Ma, H.J. Bernstein, Phys. Rev. **187**, 345 (1969); R. Dashen, S.-K. Ma, Phys. Rev. A **4**, 700 (1971).
- [12] M. I. Gorenstein, V. K. Petrov, and G. M. Zinovjev, Phys. Lett. B **106**, 327 (1981); D. H. Rischke, M. I. Gorenstein, H. Stöcker, and W. Greiner, Z. Phys. C **51**, 485 (1991).
- [13] B. D. Serot and J. D. Walecka, *Advances in Nuclear Physics* (Plenum, New York, 1986), Vol 16; Int. Journ. Mod. Phys. E **6**, 515 (1997).
- [14] O. Lourenco, M. Dutra, A. Delfino, and M. Malheiro, Phys. Rev. D **84**, 125034 (2011).
- [15] J. Cleymans, M. I. Gorenstein, J. Stalnacke, and E. Suhonen, Phys. Scripta **48**, 277 (1993).
- [16] M. I. Gorenstein, H. Stoecker, G. D. Yen, S. N. Yang, and W. Greiner, J. Phys. G **24**, 1777 (1998).
- [17] Y. Hama, T. Kodama and O. Socolowski, Jr., Braz. J. Phys. **35**, 24 (2005) [hep-ph/0407264].
- [18] K. Werner, Iu. Karpenko, T. Pierog, M. Bleicher and K. Mikhailov, Phys. Rev. C **82**, 044904 (2010) [arXiv:1004.0805 [nucl-th]].
- [19] L. M. Satarov, M. N. Dmitriev, and I. N. Mishustin, Phys. Atom. Nucl. **72**, 1390 (2009); A. V. Merdeev, L. M. Satarov, and I. N. Mishustin, Phys. Rev. C **84**, 014907 (2011).
- [20] A. Andronic, P. Braun-Munzinger, J. Stachel and M. Winn, arXiv:1201.0693 [nucl-th].
- [21] J. Randrup and J. Cleymans, Phys. Rev. C **74**, 047901 (2006).
- [22] J. Cleymans, H. Oeschler, K. Redlich, and S. Wheaton, Phys. Lett. B **615**, 50 (2005).
- [23] J. Cleymans, H. Oeschler, K. Redlich, and S. Wheaton, Phys. Rev. C **73**, 034905 (2006).
- [24] J. Cleymans, Phys. Part. Nucl. Lett., Vol. **8**, No. 8, 797 (2011).
- [25] M. Gaździcki and M. I. Gorenstein, Acta Phys. Polon. B **30**, 2705 (1999); S. V. Afanasiev *et al.* [The NA49 Collaboration], Phys. Rev. C **66**, 054902 (2002); C. Alt *et al.* [NA49 Collaboration],

- Phys. Rev. C **77**, 024903 (2008); M. Gaździcki, M. Gorenstein and P. Seyboth, Acta Phys. Polon. B **42**, 307 (2011).
- [26] A. Aduszkiewicz *et al.* [NA61 Collaboration], Acta Phys. Polon. B **43**, 635 (2012) [arXiv:1201.5879 [nucl-ex]].
- [27] G. Odyniec *et al.* [STAR Collaboration], Acta Phys. Polon. B **43**, 627 (2012).
- [28] A. N. Sissakian *et al.* [NICA Collaboration], J. Phys. G **36**, 064069 (2009); A. Sorin, V. Kekelidze, A. Kovalenko, R. Lednicky, I. Meshkov and G. Trubnikov, “Heavy-ion program at NICA/MPD at JINR,” Nucl. Phys. A **855**, 510 (2011).
- [29] B. Friman, (ed.), C. Hohne, (ed.), J. Knoll, (ed.), S. Leupold, (ed.), J. Randrup, (ed.), R. Rapp, (ed.) and P. Senger, (ed.), Lect. Notes Phys. **814**, 1 (2011).
- [30] H. Stoecker and C. Sturm, Nucl. Phys. A **855**, 506 (2011).
- [31] T. Galatyuk, *Investigation of baryon rich dense nuclear matter at SIS100*, ”CPOD-2013”, March 11-15, 2013, Napa, California, USA [<https://www-alt.gsi.de/documents/DOC-2013-Mar-43-1.pdf>].
- [32] S. Wheaton and J. Cleymans, Comput. Phys. Commun. **180**, 84 (2009) [hep-ph/0407174].
- [33] L. D. Landau and E. M. Lifshitz, Statistical Physics (Oxford: Pergamon) 1975.
- [34] M. I. Gorenstein, Phys. Rev. C **86**, 044907 (2012).
- [35] P. Braun-Munzinger, K. Redlich and J. Stachel, In \*Hwa, R.C. (ed.) et al.: Quark gluon plasma\* 491-599 [nucl-th/0304013]; P. Braun-Munzinger, I. Heppe and J. Stachel, Phys. Lett. B **465**, 15 (1999) [nucl-th/9903010].
- [36] M. I. Gorenstein, M. Hauer, and D. O. Nikolajenko, Phys. Rev. C **76**, 024901 (2007).
- [37] J. Fu, Phys. Lett. B **722**, 144 (2013).
- [38] V. V. Begun, M. Gazdzicki, M. I. Gorenstein and O. S. Zozulya, Phys. Rev. C **70**, 034901 (2004) [nucl-th/0404056]; V. V. Begun, M. Gazdzicki, M. I. Gorenstein, M. Hauer, V. P. Konchakovski and B. Lungwitz, Phys. Rev. C **76**, 024902 (2007) [nucl-th/0611075].
- [39] A. Bzdak, V. Koch and V. Skokov, Phys. Rev. C **87**, 014901 (2013) [arXiv:1203.4529 [hep-ph]]; A. Bzdak and V. Koch, Phys. Rev. C **86**, 044904 (2012) [arXiv:1206.4286 [nucl-th]].